Advanced Materials Research
ISSN: 1662-8985, Vols. 433-440, pp 3863-3869
doi:10.4028/www.scientific.net/AMR.433-440.3863 Online: 2012-01-03

Field Analysis of Ridged Waveguides USING TRANSFER MATRIX

Wei-hua Zong[1a], Ming-xin Shao[2b] and Xiao-yun Qu[3c]

[1]Shandong Provincial Key Laboratory of Industrial Control Technology,School of Automation Engineering, Qingdao University, Qingdao, China 266071

[2]Hisense Network Technology Co. Ltd., Qingdao, China 266071,

[3]China Aerospace Science and Technology Corporation No. 5 Academy No.513 , Institute, Yantai, China 264000,

Email: [a] weihuazong@126.com, [b] mxshao@126.com, [c] selina.qu@163.com

Keywords- matrices; mode matching method; ridged waveguides; transfer matrix

Abstract. The mode matching method is applied to analyze generalized ridged waveguides. The tangential fields in each region are expressed in terms of the product of several matrices, i.e., a functional matrix about x-F(x), a functional matrix about y-G(y) and a column vector of amplitudes. The boundary conditions are transformed into a set of linear equations by taking the inner products of each element of G(y) with weight functions. Two types of ridged waveguide are calculated to validate the theory. Several new modes not reported in previous analysis are presented.

Introduction

Ridged waveguides have many applications in microwave and millimeter wave devices, owing to the well known fact that the cutoff frequency of the fundamental mode is far lower than that of the rectangular waveguide with the same outer dimensions [1-3]. Theoretical research on them has been continued steadily [1,2,4-9]. The analysis methods involve mode-matching technique [1, 2, 5, 6], quasi-static method [4], variational method [7] and integral equations technique [8, 9]. All these approaches are only for the analysis of ridged waveguide with a certain structure, can not be used to analyze a group of ridged waveguides with different shapes. In this paper, a general mode matching method is presented, applying to different types of generalized ridged waveguides (shown in Figure 1). The waveguide is constructed by inserting arbitrary number of rectangular ridges in the rectangular waveguide.

To analyze the waveguide, the structure is divided into I regions. For each region i ($x_i \le x \le x_{i+1}$, $y_i \le y \le y_i + b_i$), we express the tangential fields in each region in terms of the multiplication of several matrices, *i.e.*, a functional matrix about x-$\mathbf{F}(x)$, a functional matrix about y-$\mathbf{G}(y)$ and a column vector of amplitudes of the individual region. The boundary conditions of each pair of adjacent regions are accomplished by taking the inner products of each element of $\mathbf{G}(y)$ with weight functions and a set of linear equations are obtained. While neither the eigenvalues nor the amplitudes can be solved directly from the equations. The boundary conditions of the waveguide's wall are involved to solve the problem. Two types of ridged waveguide are calculated to validate the theory. Several new modes not reported in previous analysis are presented.

Matrix Formulation Of Field Components

In general, the modes in ridged waveguide with inhomogenous dielectric filled are neither TE nor TM to the guide axis. In each region the fields can be expressed as a superposition of TE and TM modes of parallel planes. We denote $\phi_h^{(i)}$ and $\phi_e^{(i)}$ as z-components of the magnetic-type and electric-type Hertzian potentials of TE and TM modes in region i, respectively. They are assumed to be ($e^{-j\beta z}$ is omitted in this paper).

$$\phi_h^{(i)} = \sum_{n=0}^{\infty}[A_n^{(i)} \sin k_{xn}^{(i)}(x-d_i) + B_n^{(i)} \cos k_{xn}^{(i)}(x-d_i)] \cdot \cos k_{yn}^{(i)}(y-y_i) \tag{1.a}$$

$$\phi_e^{(i)} = \sum_{n=1}^{\infty}[C_n^{(i)} \sin k_{xn}^{(i)}(x-d_i) + D_n^{(i)} \cos k_{xn}^{(i)}(x-d_i)] \cdot \sin k_{yn}^{(i)}(y-y_i) \tag{1.b}$$

$$k_{yn}^{(i)} = \frac{n\pi}{b_i}, \quad n = 0,1,2\ldots \tag{2}$$

$$k_{xn}^{(i)} = \sqrt{\omega^2 \varepsilon_i \mu_0 - (k_{yn}^{(i)})^2 - \beta^2}, \quad n = 0,1,2\ldots \tag{3}$$

where the upper symbol of (i) represents region i. $A_n^{(i)}$, $B_n^{(i)}$, $C_n^{(i)}$, and $D_n^{(i)}$ are amplitude coefficients of each region. And $d_1=x_1$, $d_I=x_{I+1}$, $d_i=x_i$ (for $1<i<I$).

The amplitude coefficients are all unknown in previous

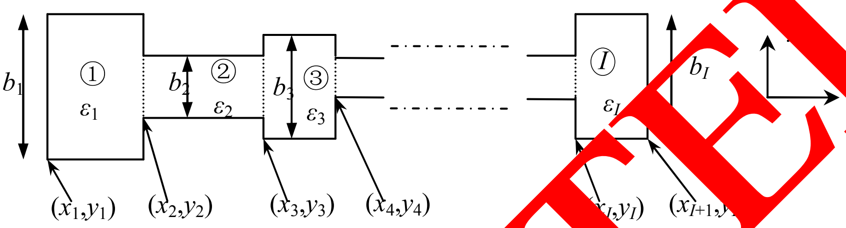

Figure 1. Cross section of rectangular waveguide with multi-ridge.

analysis. But in this paper, for regions 1 and I, some of the coefficients are of zero, determined by the boundary conditions at $x=x_1$, x_{I+1} (which is perfect electric or magnetic walls). This will be discussed in section 4.

Then the tangential field components in each region are written as follows

$$E_y^{(i)} = \sum_{n=0}^{\infty} k_{xn}^{(i)}[A_n^{(i)} \cos k_{xn}^{(i)}(x-d_i) - B_n^{(i)} \sin k_{xn}^{(i)}(x-d_i)] \cdot \cos k_{yn}^{(i)}(y-y_i) - \beta/\omega\varepsilon_i \sum_{n=1}^{\infty} k_{yn}^{(i)}[C_n^{(i)} \sin k_{xn}^{(i)}(x-d_i) + D_n^{(i)} \cos k_{xn}^{(i)}(x-d_i)] \cos k_{yn}^{(i)}(y-y_i) \tag{4.a}$$

$$E_z^{(i)} = j(\beta^2/\omega\varepsilon_i - \omega\mu_0)\sum_{n=1}^{\infty}[C_n^{(i)} \sin k_{xn}^{(i)}(x-d_i) + D_n^{(i)} \cos k_{xn}^{(i)}(x-d_i)] \sin k_{yn}^{(i)}(y-y_i) \tag{4.b}$$

$$H_y^{(i)} = (\beta/\omega\mu_0)\sum_{n=1}^{\infty}[(A_n^{(i)}k_{yn}^{(i)} + D_n^{(i)}k_{xn}^{(i)}) \sin k_{xn}^{(i)}(x-d_i) + (B_n^{(i)}k_{yn}^{(i)} - C_n^{(i)}k_{xn}^{(i)}) \cos k_{xn}^{(i)}(x-d_i)] \sin k_{yn}^{(i)}(y-y_i) \tag{4.c}$$

$$H_z^{(i)} = j(\beta^2/\omega\mu_0 - \omega\varepsilon_i)\sum_{n=0}^{\infty}[(A_n^{(i)} \sin k_{xn}^{(i)}(x-d_i) + B_n^{(i)} \cos k_{xn}^{(i)}(x-d_i)] \cos k_{yn}^{(i)}(y-y_i) \tag{4.d}$$

Because of the limitation of computing time and storage requirements, the infinite series terms in (4) are restricted to finite number N_i. The expression in (4) can be written in matrix notation as

$$\begin{bmatrix} E_y^{(i)} \\ E_z^{(i)} \\ H_y^{(i)} \\ jH_z^{(i)} \end{bmatrix} = \mathbf{G}^{(i)}(y)\mathbf{F}^{(i)}(x)\begin{bmatrix} \mathbf{A}^{(i)} \\ \mathbf{B}^{(i)} \\ \mathbf{C}^{(i)} \\ \mathbf{D}^{(i)} \end{bmatrix} \tag{5}$$

where

$$\mathbf{A}^{(i)} = \begin{bmatrix} A_0^{(i)} \\ \vdots \\ A_{N_i}^{(i)} \end{bmatrix}, \mathbf{B}^{(i)} = \begin{bmatrix} B_0^{(i)} \\ \vdots \\ B_{N_i}^{(i)} \end{bmatrix}, \mathbf{C}^{(i)} = \begin{bmatrix} C_1^{(i)} \\ \vdots \\ C_{N_i}^{(i)} \end{bmatrix}, \quad \mathbf{D}^{(i)} = \begin{bmatrix} D_1^{(i)} \\ \vdots \\ D_{N_i}^{(i)} \end{bmatrix}$$

The components of $\mathbf{G}^{(i)}(y)$ and $\mathbf{F}^{(i)}(x)$ are as follows

$$\mathbf{G}^{(i)}(y) = \begin{bmatrix} \mathbf{G}_1^{(i)}(y) & \mathbf{0} & \mathbf{0} & \mathbf{0} \\ \mathbf{0} & \mathbf{G}_2^{(i)}(y) & \mathbf{0} & \mathbf{0} \\ \mathbf{0} & \mathbf{0} & \mathbf{G}_3^{(i)}(y) & \mathbf{0} \\ \mathbf{0} & \mathbf{0} & \mathbf{0} & \mathbf{G}_4^{(i)}(y) \end{bmatrix}_{4\times(4N_i+2)}$$

$$
\mathbf{F}^{(i)}(x)=\begin{bmatrix}
\mathbf{F}_{11}^{(i)}(x) & \mathbf{F}_{12}^{(i)}(x) & \mathbf{F}_{13}^{(i)}(x) & \mathbf{F}_{14}^{(i)}(x)\\
\mathbf{F}_{21}^{(i)}(x) & \mathbf{F}_{22}^{(i)}(x) & \mathbf{F}_{23}^{(i)}(x) & \mathbf{F}_{24}^{(i)}(x)\\
\mathbf{F}_{31}^{(i)}(x) & \mathbf{F}_{32}^{(i)}(x) & \mathbf{F}_{33}^{(i)}(x) & \mathbf{F}_{34}^{(i)}(x)\\
\mathbf{F}_{41}^{(i)}(x) & \mathbf{F}_{42}^{(i)}(x) & \mathbf{F}_{43}^{(i)}(x) & \mathbf{F}_{44}^{(i)}(x)
\end{bmatrix}_{(4N_i+2)\times(4N_i+2)} \tag{7}
$$

where $diag(f_n)_{n\in[n_{\min},n_{\max}]}$ means a diagonal square matrix with element f_n for $n=n_{\min},n_{\min}+1,\cdots,n_{\max}$.

Field Matching

We define

$$
i_+=\begin{cases} i & if \quad b_i\ge b_{i-1}\\ i-1 & if \quad b_i<b_{i-1}\end{cases},\ i_-=\begin{cases} i-1 & if \quad b_i\ge b_{i-1}\\ i & if \quad b_i<b_{i-1}\end{cases} \tag{8}
$$

then the boundary conditions at $x=x_i(i=2,3,\ldots,I)$ are given by

$$
E_y^{(i_+)}(x_i)=\begin{cases} 0 & y\in[y_{i_+},y_{i_+}+b_{i_+}]/[y_{i_-},y_{i_-}+b_{i_-}]\\ E_y^{(i_-)}(x_i) & y\in[y_{i_-},y_{i_-}+b_{i_-}]\end{cases} \tag{9.a}
$$

$$
E_z^{(i_+)}(x_i)=\begin{cases} 0 & y\in[y_{i_+},y_{i_+}+b_{i_+}]/[y_{i_-},y_{i_-}+b_{i_-}]\\ E_z^{(i_-)}(x_i) & y\in[y_{i_-},y_{i_-}+b_{i_-}]\end{cases} \tag{9.b}
$$

$$
H_y^{(i)}(x_i)=H_y^{(i-1)}(x_i),\ y\in[y_{i_-},y_{i_-}+b_{i_-}] \tag{9.c}
$$

$$
H_z^{(i)}(x_i)=H_z^{(i-1)}(x_i),\quad y\in[y_{i_-},y_{i_-}+b_{i_-}] \tag{9.d}
$$

To transform the boundary conditions into an algebraic system, we take the inner products of both sides of (9) with weight functions. Usually the eigenfunctions of the guide with larger height are chosen as the weight functions for enforcing the electric continuity in (9.a) and (9.b), and the eigenfunctions of the smaller guide are chosen for magnetic continuity in (9.c) and (9.d).

Taking the inner products of both sides of (9.a-d) with $\mathbf{W}_1^{(i)}(y)$, $\mathbf{W}_2^{(i)}(y)$, $\mathbf{W}_3^{(i)}(y)$ and $\mathbf{W}_4^{(i)}(y)$, respectively, we can get matching equations. Considering the matrix form of fields in (5), the above process can be accomplished by taking the inner products of each element of $\mathbf{G}^{(i-1)}(y)$ and $\mathbf{G}^{(i)}(y)$ with same weight functions. The result can be written as

$$
\hat{\mathbf{G}}^{(i,i)}\mathbf{F}^{(i)}(x_i)\begin{bmatrix}\mathbf{A}^{(i)}\\ \mathbf{B}^{(i)}\\ \mathbf{C}^{(i)}\\ \mathbf{D}^{(i)}\end{bmatrix}=\hat{\mathbf{G}}^{(i,i-1)}\mathbf{F}^{(i-1)}(x_i)\begin{bmatrix}\mathbf{A}^{(i-1)}\\ \mathbf{B}^{(i-1)}\\ \mathbf{C}^{(i-1)}\\ \mathbf{D}^{(i-1)}\end{bmatrix},\quad i=2,3,\cdots,I \tag{10}
$$

$$
\hat{\mathbf{G}}^{(i,j)}=\begin{bmatrix}\hat{\mathbf{G}}_1^{(i,j)} & \mathbf{0} & \mathbf{0} & \mathbf{0}\\ \mathbf{0} & \hat{\mathbf{G}}_2^{(i,j)} & \mathbf{0} & \mathbf{0}\\ \mathbf{0} & \mathbf{0} & \hat{\mathbf{G}}_3^{(i,j)} & \mathbf{0}\\ \mathbf{0} & \mathbf{0} & \mathbf{0} & \hat{\mathbf{G}}_4^{(i,j)}\end{bmatrix},\quad j=i,i-1 \tag{11}
$$

$$
\hat{\mathbf{G}}_k^{(i,j)}=\int \mathbf{W}_k^{(i)}(y)\mathbf{G}_k^{(j)}(y)dy,\quad k=1,2,3,4 \tag{12}
$$

where i represents $x=x_i$, j represents the region j.

Eigenvalue Equation

The eigenvalues and unknown amplitudes cannot be solved directly from the linear equations of (10), because the number of equation is less than that of the amplitude. The boundary conditions at $x=x_1$, x_{I+1} are used to determine the eigenvalues and amplitudes.

Let $N_i\equiv N$ (i=1,2, …,I), then $\hat{\mathbf{G}}^{(i,i)}\mathbf{F}^{(i)}(x_i)$ is a square matrix. By calculating the inverse of $\hat{\mathbf{G}}^{(i,i)}\mathbf{F}^{(i)}(x_i)$ in (10), we get

$$\begin{bmatrix} \mathbf{A}^{(i)} \\ \mathbf{B}^{(i)} \\ \mathbf{C}^{(i)} \\ \mathbf{D}^{(i)} \end{bmatrix} = [\mathbf{F}^{(i)}(x_i)]^{-1}[\hat{\mathbf{G}}^{(i,i)}]^{-1}\hat{\mathbf{G}}^{(i,i-1)}\mathbf{F}^{(i-1)}(x_i) \begin{bmatrix} \mathbf{A}^{(i-1)} \\ \mathbf{B}^{(i-1)} \\ \mathbf{C}^{(i-1)} \\ \mathbf{D}^{(i-1)} \end{bmatrix} \tag{13}$$

Let

$$\mathbf{T}^{(i)} = [\mathbf{F}^{(i)}(x_i)]^{-1}[\hat{\mathbf{G}}^{(i,i)}]^{-1}\hat{\mathbf{G}}^{(i,i-1)}\mathbf{F}^{(i-1)}(x_i) \tag{14}$$

$\mathbf{T}^{(i)}$ is the transfer matrix considering higher order modes for the region i. When cascading the transfer matrix of every pair of adjacent regions, we get

$$\begin{bmatrix} \mathbf{A}^{(i)} \\ \mathbf{B}^{(i)} \\ \mathbf{C}^{(i)} \\ \mathbf{D}^{(i)} \end{bmatrix} = \mathbf{T}^{(i)} \begin{bmatrix} \mathbf{A}^{(i-1)} \\ \mathbf{B}^{(i-1)} \\ \mathbf{C}^{(i-1)} \\ \mathbf{D}^{(i-1)} \end{bmatrix} = \mathbf{T}^{(i)}\mathbf{T}^{(i-1)}\cdots\mathbf{T}^{(2)} \begin{bmatrix} \mathbf{A}^{(1)} \\ \mathbf{B}^{(1)} \\ \mathbf{C}^{(1)} \\ \mathbf{D}^{(1)} \end{bmatrix} = \mathbf{M}^{(i)} \begin{bmatrix} \mathbf{A}^{(1)} \\ \mathbf{B}^{(1)} \\ \mathbf{C}^{(1)} \\ \mathbf{D}^{(1)} \end{bmatrix} \tag{15}$$

The amplitudes in the region i are expressed in terms of the amplitudes of the region 1. To perform calculation of eigenvalues, we express $\mathbf{M}^{(i)}$ with several submatrices

$$\mathbf{M}^{(i)} = \begin{bmatrix} \mathbf{M}_{11}^{(i)} & \mathbf{M}_{12}^{(i)} & \mathbf{M}_{13}^{(i)} & \mathbf{M}_{14}^{(i)} \\ \mathbf{M}_{21}^{(i)} & \mathbf{M}_{22}^{(i)} & \mathbf{M}_{23}^{(i)} & \mathbf{M}_{24}^{(i)} \\ \mathbf{M}_{31}^{(i)} & \mathbf{M}_{32}^{(i)} & \mathbf{M}_{33}^{(i)} & \mathbf{M}_{34}^{(i)} \\ \mathbf{M}_{41}^{(i)} & \mathbf{M}_{42}^{(i)} & \mathbf{M}_{43}^{(i)} & \mathbf{M}_{44}^{(i)} \end{bmatrix} \tag{16}$$

Considering boundary conditions at $x=x_1$ and $x=x_{I+1}$, we have

$$\begin{bmatrix} \mathbf{M}_{12}^{(I)} & \mathbf{M}_{13}^{(I)} \\ \mathbf{M}_{42}^{(I)} & \mathbf{M}_{43}^{(I)} \end{bmatrix} \begin{bmatrix} \mathbf{B}^{(1)} \\ \mathbf{C}^{(1)} \end{bmatrix} = \mathbf{0} \tag{17}$$

The above equations will have a nontrivial solution if and only if

$$\begin{vmatrix} \mathbf{M}_{12}^{(I)} & \mathbf{M}_{13}^{(I)} \\ \mathbf{M}_{42}^{(I)} & \mathbf{M}_{43}^{(I)} \end{vmatrix} = 0 \tag{18}$$

Equation (18) is the eigenvalue equation.

Numerical Results

Two examples are calculated to validate the theory.

Ridged Waveguide with Inhomogeneous Dielectric-Slab loading. The waveguide is shown in Figure 2. It has an aspect ratio of b/a=0.5 and a dielectric slab of cross-sectional dimensions a' and b' is placed inside the gap between the ridges, whereas the outer parts of the waveguide's cross section remain empty. Figure 3 shows gap-height dependence of the cutoff wavelength λ_c of the dominant mode normalized to the waveguide broad dimension a with a'=0.5a. The permittivity ε_r severs as parameter. The solid line is obtained with N=5 and the dots are from [6]. We can see in Fig.3 that the data agree well with those in [6].

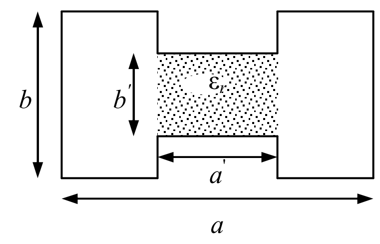

Figure 2. Cross section of ridged waveguide with inhomogeneous dielectric-slab loading

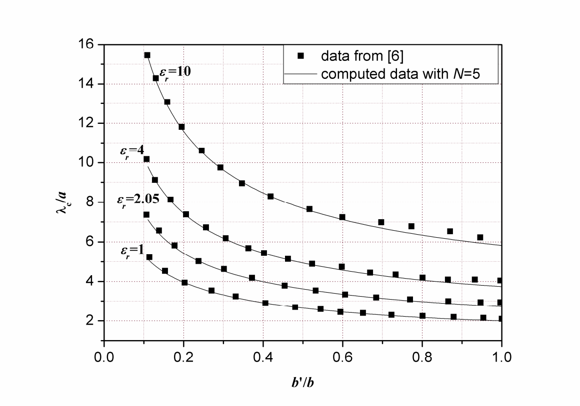

Figure 3. Gap-height dependence of cutoff wavelength λc of the dominant mode normalized to the waveguide broad dimension a

Single-Ridged Waveguide. The waveguide is filled with air, with dimensions of a=b=9.5 mm, s=0.15 mm, and d=1.7 mm (see Figure 4). Using the symmetry of the waveguide, the modes can be classified into two types: 1) odd modes with a perfect magnetic wall at x=0; 2) even modes with a perfect electric wall at x=0. We call the kth odd mode as mode 2k-1, and the kth even mode as mode 2k (k=1,2,3…).

Tables 1 and 2 show the cutoff wavenumbers of the first eleven modes of even and odd modes respectively, along with the data presented in [7, 8]. The waveguide is studied in [7, 8] by use of variational method and integral equations technique respectively, whereas only odd modes are considered in [7].

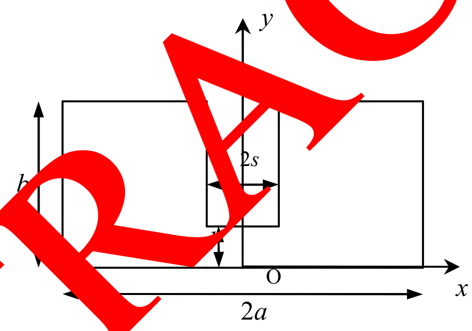

Figure 4. Cross section of single-ridged waveguide

As shown in Table 1, the agreement is good, except for mode 19. The calculated result of mode 19 is similar to that of TM mode 5 in Table III of [8], whereas the datum is absent in [7]. In Table 2, the computed data of even mode have much difference from [8]. There are corresponding data in [8] for mode 16, 20 and 22, while no data for other modes are presented in [8]. It is found that the first higher order mode is an even mode and its cutoff number is 0.3297, different from the value of 0.3332 in [8].

TABLE I. CUTOFF WAVENUMBERS (RAD/MM) OF THE FIRST ODD ODD MODES IN A SINGLE-RIDGE WAVEGUIDES

Mode m	Present Method (N=10)	Ref. [7]	Ref. [8]
1	0.0938	0.093	0.0926
3	0.3332	0.3332	0.3332
5	0.3817	0.3881	0.3811
7	0.4710	0.4665	0.4711
9	0.5277	0.5265	0.5263
11	0.6654	0.6654	0.6653
13	0.6916	0.6913	0.6916
15	0.7407	0.7358	0.7410
17	0.7457	0.7456	0.7453
19	0.7480		0.7481
21	0.831417	0.8298	0.8295

TABLE II. CUTOFF WAVENUMBERS (RAD/MM) OF THE FIRST ELEVEN ODD MODES IN A SINGLE-RIDGE WAVEGUIDES

Mode m	Present Method (N=10)	Ref. [7]
2	0.3297	
4	0.3352	
6	0.4691	
8	0.4713	[illegible]
10	[illegible]	
12	[illegible]	
14	[illegible]	
16	[illegible]	0.7416
[illegible]	0.7465	
20	0.7487	0.7487

Conclusions

The advantage of the approach is that the formulations can be used to analyze ridged waveguides with any shape and the matching equations can be easily got from boundary conditions by simple matrix operation.

Acknowledgments

The work of Wei-hua Zong was supported in part by Shandong Provincial Education Department, P. R. China under the International Cooperation Program for Excellent Lectures of 2009.

References

[1] M. M. Fahmi, J. A. Ruiz-Crusz, R. R. Mansour, K. A. Zaki, “Compact ridge waveguide filter with arbitrarily placed transmission zeros using nonresonating nodes”, IEEE Trans. Microwave Theory Tech, vol. 57, pp. 3354-3360, Dec., 2009.

[2] Ruiz-Cruz, J. A.; Zhang, Y.; Zaki, K. A.; Piloto, A. J.; Tallo, J., “Ultra-Wideband LTCC Ridge Waveguide Filters”, IEEE Microwave and Wireless Components Letters, vol. 17, pp. 115-117, March, 2007.

[3] S. Bastioli, L. Marcaccioli, R. Sorrentino, “Waveguide Pseudoelliptic Filters Using Slant and Transverse Rectangular Ridge Resonators”, IEEE Trans. Microw. Theory Tech., vol. 56, pp. 3129-3136, Dec., 2008.

[4] Y. Rong and K.A. Zaki, “Characteristics of generalized rectangular and circular waveguides”, IEEE Trans. Microw. Theory Tech., vol. 48, pp. 258-264, March, 2000.

[5] G. Magerl, “Ridged waveguides with inhomogeneous dielectric slab loading”, IEEE Trans. Microw. Theory Tech., vol. 26, pp. 413-416, June, 1978.

[6] Y. Utsumi, “Variational analysis of ridged waveguide modes”, IEEE Trans. Microw. Theory Tech., vol. 33, pp. 111-120, Feb. 1985.

[7] S. Amari, I. Bornemann and R. Vahldieck, “Application of a Coupled-Integral-Equations Technique to ridged waveguide”, IEEE Trans. Microwave Theory Tech., vol. 44, pp. 2256-2264, Dec. 1996.

[8] W. Sun and C. A. Balanis, “MFIE analysis and design of ridged waveguides”, *IEEE Trans. Microw. Theory Tech.*, vol. 41, pp. 1965-1971, Nov. 1993.